Available online at www.sciencedirect.com
ScienceDirect
Journal of Organometallic Chemistry 693 (2008) 601–610
Journal of Organometallic Chemistry
www.elsevier.com/locate/jorganchem

Synthesis, characterization and catalytic behaviour of *ansa*-zirconocene complexes containing tetraphenylcyclopentadienyl rings: X-ray crystal structures of $[Zr\{Me_2Si(\eta^5\text{-}C_5Ph_4)(\eta^5\text{-}C_5H_3R)\}Cl_2]$ (R = H, Bu^t)

Santiago Gómez-Ruiz [a,b], Dorian Polo-Cerón [a], Sanjiv Prashar [a,*], Mariano Fajardo [a], Víctor L. Cruz [c], Javier Ramos [c], Evamarie Hey-Hawkins [b]

[a] *Departamento de Química Inorgánica y Analítica, E.S.C.E.T., Universidad Rey Juan Carlos, 28933 Móstoles (Madrid), Spain*
[b] *Institut für Anorganische Chemie der Universität Leipzig, Johannisallee 29, D-04103 Leipzig, Germany*
[c] *Instituto de Estructura de la Materia, CSIC, Serrano, 113bis, E-28006, Madrid, Spain*

Received 29 August 2007; received in revised form 2 November 2007; accepted 19 November 2007
Available online 5 December 2007

Abstract

The *ansa*-bis(cyclopentadiene) compounds, $Me_2Si(C_5HPh_4)(C_5H_4R)$ (R = H (**2**); Bu^t (**3**)), have been prepared by the reaction of $C_5HPh_4(SiMe_2Cl)$ (**1**) with $Na(C_5H_5)$ or $Li(C_5H_4Bu^t)$, respectively, and transformed to the di-lithium derivatives, $Li_2\{Me_2Si(C_5Ph_4)(C_5H_3R)\}$ (R = H (**4**); Bu^t (**5**)), by the action of *n*-butyllithium. The *ansa*-zirconocene complexes, $[Zr\{Me_2Si(\eta^5\text{-}C_5Ph_4)(\eta^5\text{-}C_5H_3R)\}Cl_2]$ (R = H (**6**); Bu^t (**7**)), were synthesized from the reaction of $ZrCl_4$ with **4** or **5**, respectively. Compounds **6** and **7** have been tested in the polymerization of ethylene and compared with their methyl-substituted analogues, $[Zr\{Me_2Si(\eta^5\text{-}C_5Me_4)(\eta^5\text{-}C_5H_3R)\}Cl_2]$ (R = H (**8**); Bu^t (**9**)). Whilst **8** and **9** are catalytically active, the tetraphenyl-substituted complexes **6** and **7** proved to be inactive in the polymerization of ethylene. This phenomenon has been explained by DFT calculations based on the reaction intermediates in the polymerization processes involving **6** and **7**, which showed that the extraction of a methyl group from the zirconocene complex to form the cationic active specie is endothermic and therefore unfavourable.

Keywords: *ansa*-Metallocene; Zirconium; Tetraphenylcyclopentadienyl; Polymerization; DFT calculations

1. Introduction

Taking into account that metallocene complexes are amongst those most studied in the field of organometallic chemistry [1], it is therefore surprising that only a handful of compounds containing tetraphenylcyclopentadienyl or pentaphenylcyclopentadienyl ligands have been reported [2]. These reports have shown that the presence of these bulky cyclopentadienyl ligands greatly reduce the reactivity of their complexes, when compared with the unsubstituted metallocene analogues [2]. Solid-state and solution studies have allowed a greater understanding of the influence of the phenyl groups and of the interaction between and within the cyclopentadienyl rings of the metallocene complex [2,3]. Further work dealing with the stability and conformation of bis(tetraphenylcyclopentadienyl) metal complexes, such as $[M(\eta^5\text{-}C_5HPh_4)_2]$ (M = V, Cr, Co, and Ni), has also been carried out although the bent metallocene conformation was never observed [2]. Nevertheless, in the case of the group four metals, the bent metallocene conformation was easily accessible although the reactivity of these complexes was limited [2,4]. In particular, for zirconium, only a few metallocene complexes incorporating the tetraphenylcyclopentadienyl have been described [4,5].

* Corresponding author. Tel.: +34 914887186; fax: +34 914888143.
E-mail address: sanjiv.prashar@urjc.es (S. Prashar).

0022-328X/$ - see front matter © 2007 Elsevier B.V. All rights reserved.
doi:10.1016/j.jorganchem.2007.11.054

Considering that the catalytic activity and selectivity in olefin polymerization is directly influenced by the structure of the metallocene complex [6] and as a continuation of our work in the molecular architecture of metallocene complexes and their application as catalysts in the polymerization of olefins [7], we present here the synthesis and structural characterization of *ansa*-zirconocene complexes with tetraphenylcyclopentadienyl rings. We also report our findings on the lack of catalytic activity of **6** and **7** in the polymerization of ethylene which we explain on the basis of DFT calculations of the possible catalytically active species.

2. Results and discussion

The reaction of $Li(C_5HPh_4)$ with an excess (1:3) of Cl_2SiMe_2 led to the formation of $C_5HPh_4(SiMe_2Cl)$ (**1**) (Scheme 1) which was characterized by ^1H NMR spectroscopy and mass spectrometry. The preparation of the asymmetrically substituted *ansa* ligand precursors, $Me_2Si(C_5HPh_4)(C_5H_4R)$ (R = H (**2**); R = Bu^t (**3**)), was achieved by the reaction of **1** with $Na(C_5H_5)$ or $Li(C_5H_4\text{-}Bu^t)$, respectively, following previously reported synthetic protocols (Scheme 1) [7a,7b]. Compounds **2** and **3** were isolated as mixtures of their double bond position isomers, with one isomer being predominant as confirmed by ^1H NMR spectroscopy. In addition, **2** and **3** were characterized by electron impact mass spectrometry (see Section 4). The *ansa*-bis(cyclopentadiene) compounds, **2** and **3**, were lithiated in the traditional manner with *n*-butyllithium to give the di-lithium derivatives $Li_2\{Me_2Si(C_5Ph_4)(C_5H_3R)\}$ (R = H (**4**); Bu^t (**5**)). The *ansa*-metallocene complexes $[Zr\{Me_2Si(\eta^5\text{-}C_5Ph_4)(\eta^5\text{-}C_5H_3R)\}Cl_2]$ (R = H (**6**); Bu^t (**7**)) were prepared by the reaction of one molar equivalent of **4** or **5** with $ZrCl_4$ in refluxing THF during 16 h (Scheme 1).

Compounds **6** and **7** were isolated as crystalline solids and characterized spectroscopically. The ^1H NMR spectrum for **6** showed the expected signals for the C_s symmetric complex. Thus, for the cyclopentadienyl ring protons two multiplets corresponding to the AA′BB′ system were observed at 5.02 and 5.48 ppm. The methyl groups of the *ansa* bridging unit are equivalent and gave a unique signal at 0.16 ppm. The introduction of a *tert*-butyl substituent changes the molecule symmetry from C_s in **6** to C_1 in **7** and this is reflected in the ^1H NMR spectrum which showed three multiplets, at 5.80, 5.93 and 6.96 ppm for the protons of the alkyl-substituted C_5 ring and two singlets, at 0.14 and 0.62 ppm, corresponding to the now inequivalent methyl groups of the $SiMe_2$ moiety. In the spectra of both **6** and **7**, a set of multiplets corresponding to the protons of the phenyl groups were observed between 7.0 and 7.2 ppm. $^{13}C\{^1H\}$ NMR spectra of **6** and **7** exhibited the expected signals (see Section 4).

The molecular structure of **6** and **7** were established by single-crystal X-ray diffraction studies. Complex **6** crystallizes in the triclinic $P\bar{1}$ space group with two molecules in the unit cell whilst **7** crystallizes in the monoclinic $P2_1/n$ space group with four molecules located in the unit cell. The molecular structure and atomic numbering scheme of **6** and **7** are shown in Figs. 1 and 2, respectively. Selected bond lengths and angles for **6** and **7** are given in Table 1.

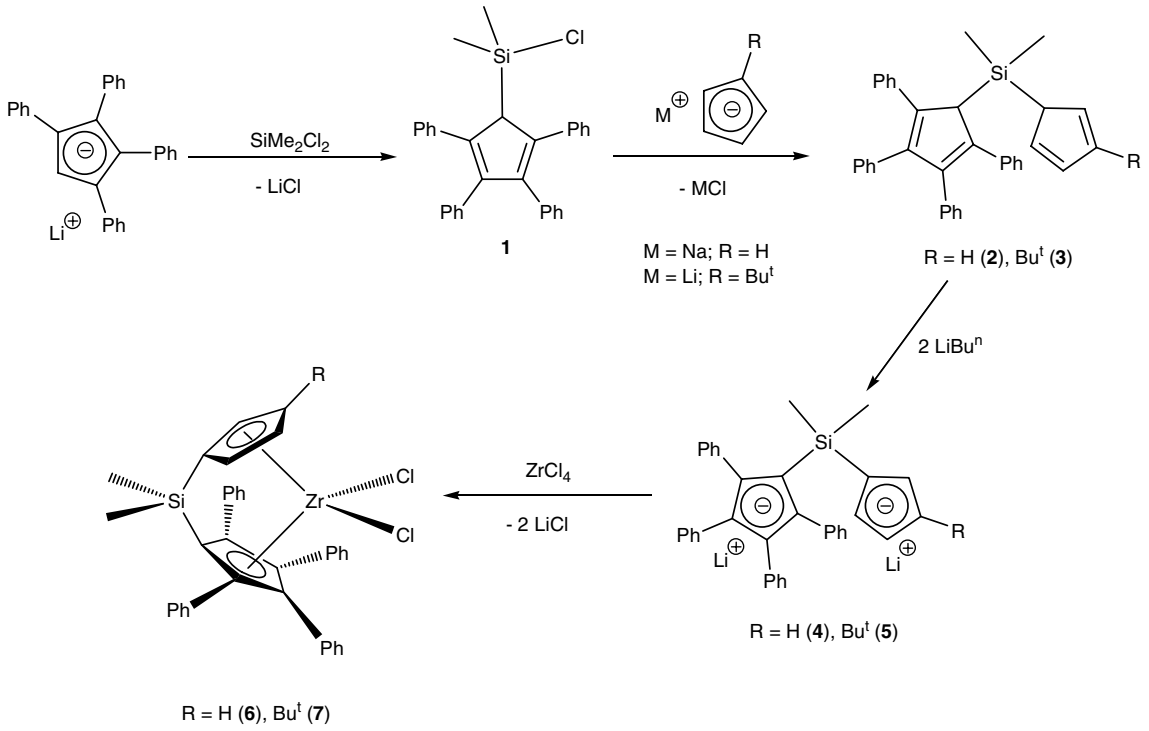

Scheme 1.

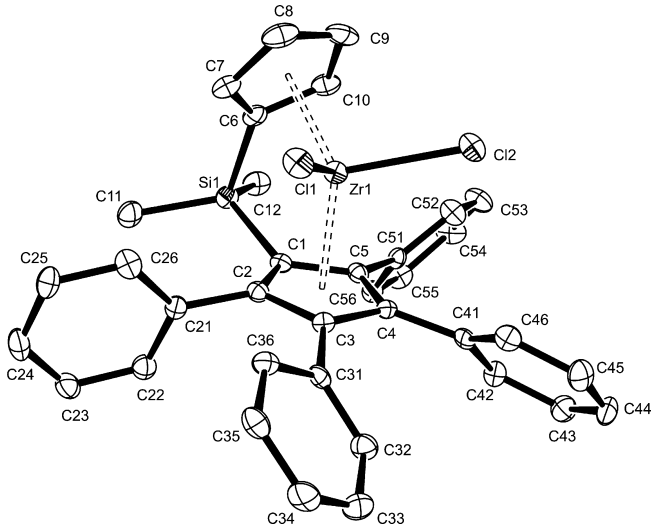

Fig. 1. Molecular structure and atom-labeling scheme for [Zr{$Me_2Si(\eta^5$-$C_5Ph_4)(\eta^5$-$C_5H_4)$}Cl_2] (**6**), with thermal ellipsoids at 50% probability.

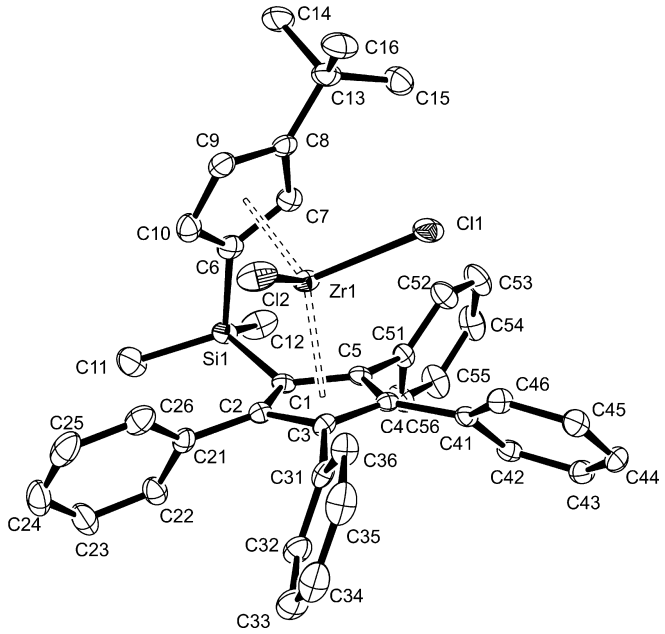

Fig. 2. Molecular structure and atom-labeling scheme for [Zr{$Me_2Si(\eta^5$-$C_5Ph_4)(\eta^5$-$C_5H_3Bu^t)$}Cl_2] (**7**), with thermal ellipsoids at 50% probability.

In addition, Table 2 contains a comparison of selected bond lengths and angles of some related zirconocene complexes.

The molecular structures of **6** and **7** reveal that the zirconium atom has a distorted tetrahedral geometry with both C_5 rings bound to the metal atom in an η^5 mode. The average Zr–C distance to the tetraphenylcyclopentadienyl ring (257.3(3) pm for **6** and 257.0(3) pm for **7**) is slightly longer than that to the other cyclopentadienyl ring (251.2(3) pm in **6** and 252.9(3) pm in **7**. This difference is more pronounced in the unbridged metallocene complex, [Zr(η^5-C_5H_5)(η^5-C_5Ph_5)Cl_2] (Zr–C[C_5Ph_5] 260.4 and Zr–C[C_5H_5] 251.2 pm) [5f]. This contrasts with the fact that

Table 1
Selected bond lengths (pm) and angles (°) for **6** and **7**

	6	**7**
Zr–Cent(1)	226.7(4)	226.6(4)
Zr–Cent(2)	220.6(4)	222.4(4)
av Zr–C(C(1)–C(5))[a]	257.3(3)	257.0(3)
av Zr–C(C(6)–C(10)))[a]	251.2(3)	252.9(3)
Zr–C(1)	250.7(3)	250.6(3)
Zr–C(2)	253.0(2)	254.0(3)
Zr–C(3)	264.6(2)	263.6(3)
Zr–C(4)	264.0(2)	264.1(3)
Zr–C(5)	254.3(2)	253.3(3)
Zr–C(6)	247.8(2)	245.7(3)
Zr–C(7)	248.6(3)	250.4(3)
Zr–C(8)	256.3(3)	265.7(3)
Zr–C(9)	256.2(2)	257.5(3)
Zr–C(10)	246.9(2)	245.4(3)
Zr–Cl(1)	242.6(1)	241.9(2)
Zr–Cl(2)	242.8(2)	243.4(2)
Cent(1)–Zr–Cent(2)	125.8(2)	126.4(2)
Si(1)–C(1)–Cent(1)	163.2(2)	162.0(2)
Si(1)–C(6)–Cent(2)	163.4(2)	165.1(2)
C(1)–Si(1)–C(11)	113.5(1)	115.7(2)
C(1)–Si(1)–C(6)	93.6(2)	94.4(2)
C(1)–Si(1)–C(12)	118.0(2)	115.7(2)
C(6)–Si(1)–C(11)	114.0(2)	109.5(2)
C(6)–Si(1)–C(12)	107.3(1)	111.4(2)
Cl(1)–Zr–Cent(1)	110.0(2)	107.3(2)
Cl(1)–Zr–Cent(2)	104.8(2)	109.5(2)
Cl(2)–Zr–Cent(1)	108.8(2)	109.3(2)
Cl(2)–Zr–Cent(2)	107.9(2)	105.8(2)
Cl(1)–Zr–Cl(2)	95.40(4)	93.65(4)

Cent(1) and Cent(2) are the centroids of C(1)–C(5) and C(6)–C(10), respectively.

[a] Refers to the average bond distance between Zr(1) and the carbon atoms of the C_5 ring of the corresponding cyclopentadienyl moiety.

essentially no difference in the average Zr–C distances between the two cyclopentadienyl rings was reported for the tetramethyl-substituted *ansa*-complexes, [Zr{$Me_2Si(\eta^5$-$C_5Me_4)(\eta^5$-$C_5H_3R)$}Cl_2] (Table 2).

For **7**, the distance from the metal to the *tert*-butyl-substituted carbon atom of the cyclopentadienyl ring, Zr(1)–C(8), is 265.7(3) pm. This bond length is significantly longer than those observed between the zirconium atom and the other carbon atoms of the cyclopentadienyl ring positioned β to the carbon atom linked to the *ansa* bridging unit [Zr(1)–C(9) 257.5(3) pm for **7** and Zr(1)–C(8) 256.3(3) and Zr(1)–C(9) 256.2(2) pm for **6**]. In the previously described *ansa*-complex, [Zr{$Me_2Si(\eta^5$-$C_5Me_4)(\eta^5$-$C_5H_3Pr^i)$}-Cl_2], the two β-carbon atoms, both substituted and unsubstituted, are located at virtually the same distance to the metal centre [7b].

The zirconium centroid distance for the tetraphenylcyclopentadienyl ring (Zr–Cent(1) 226.7(4) pm for **6** and 226.6(4) pm for **7**) is only ca. 5 pm longer than the distance between the zirconium and the centroid of the other cyclopentadienyl ring (Zr–Cent(2) 220.6(4) pm for **6** and 222.4(4) pm for **7**). For the tetramethyl-substituted *ansa*-complexes similar zirconium–centroid distances to the

Table 2
Selected structural data of some zirconocene complexes

Complex	Zr–Cp (pm)[a]	Zr–Cl (pm)	Cp–Zr–Cp (°)	Cl–Zr–Cl (°)	$C_{(cp)}$–Si–$C_{(cp)}$ (°)	Reference
$[Zr\{Me_2Si(\eta^5\text{-}C_5Ph_4)(\eta^5\text{-}C_5H_4)\}Cl_2]$ (**6**)	220.6 Cp 226.7 Cp^*	242.6(1) 242.8(1)	125.8	95.40(4)	93.6(2)	This work
$[Zr\{Me_2Si(\eta^5\text{-}C_5Me_4)(\eta^5\text{-}C_5H_4)\}Cl_2]$	220.2 Cp 219.8 Cp^*	2.451(1)	128.1	104.60(7)	95.2(2)	[7a]
$[Zr\{Me_2Si(\eta^5\text{-}C_5Ph_4)(\eta^5\text{-}C_5H_3Bu^t)\}Cl_2]$ (**7**)	222.4 Cp^R 226.6 Cp^*	241.9(2) 243.4(2)	126.4	93.65(4)	94.4(2)	This work
$[Zr\{Me_2Si(\eta^5\text{-}C_5Me_4)(\eta^5\text{-}C_5H_3Me)\}Cl_2]$	219.4 Cp^R 218.4 Cp^*	2.414(4)	126.25	101.1(2)	92.4(8)	[7a]
$[Zr\{Me_2Si(\eta^5\text{-}C_5Me_4)(\eta^5\text{-}C_5H_3Et)\}Cl_2]$	221.4 Cp^R 220.7 Cp^*	2.429(4)	126.5	100.4(2)	93.3(7)	[7b]
$[Zr\{Me_2Si(\eta^5\text{-}C_5Me_4)(\eta^5\text{-}C_5H_3Pr^i)\}Cl_2]$	222.3 Cp^R 223.0 Cp^*	2.429(4)	126.9	98.2(1)	94.2(2)	[7b]
R-$[Zr\{Me_2Si(\eta^5\text{-}C_5Me_4)(\eta^5\text{-}C_5H_3(menthyl))\}Cl_2]$		2.419(3)	126.6	98.6(2)	93.6(4)	[8]
R,*S*′-$[Zr\{Me_2Si(\eta^5\text{-}C_5Me_4)(\eta^5\text{-}C_5H_3(CHBu^tMe))\}Cl_2]$	222.7 Cp^R 222.0 Cp^*	2.4301	126.8	96.03(2)	94.25(8)	[7f]
R,*R*′-$[Zr\{Me_2Si(\eta^5\text{-}C_5Me_4)(\eta^5\text{-}C_5H_3(CHBu^tPh))\}Cl_2]$	223.2 Cp^R 221.5 Cp^*	2.4321	127.6	102.37(3)	94.11(13)	[7f]
$[Zr\{Me_2Si(\eta^5\text{-}C_5Me_4)_2\}Cl_2]$	232.9 Cp^*	2.4334(7)	128.6	99.28(3)	95.7(1)	[9]
$[Zr\{CHPhCH_2(\eta^5\text{-}C_5Ph_4)(\eta^5\text{-}C_5H_4)\}Cl_2]$	221.4 Cp 227.4 Cp^*	2.429 2.429	124.6	95.2(2)		[5c]
$[Zr(\eta^5\text{-}C_5H_5)(\eta^5\text{-}C_5Ph_5)Cl_2]$	221.1 Cp 230.2 Cp^*	2.420	132.9	96.9(2)		[5f]

[a] Cp^* refers to the C_5Me_4, C_5Ph_4 or C_5Ph_5 moiety; Cp^R refers to the C_5H_3R moiety; Cp refers to the C_5H_4 or C_5H_5 moiety.

two distinct cyclopentadienyl units were observed (Table 2). The difference in zirconium–centroid distances is greatest for the unbridged metallocene complex, $[Zr(\eta^5\text{-}C_5H_5)(\eta^5\text{-}C_5Ph_5)Cl_2]$ (Zr–Cent[C_5H_5] 221.1 and Zr–Cent[C_5Ph_5] 230.2 pm) [5f]. This fact suggests that, in the case of the rigid geometry of *ansa*-metallocene complexes, the influence of the tetraphenylcyclopentadienyl ring on the structural disposition of the molecule is less than that in the case of the unbridged metallocene complex.

The Cent(1)–Zr(1)–Cent(2) angles of 125.8° and 126.4° for **6** and **7**, respectively, are similar to those reported for other *ansa*-zirconocene complexes (Table 2). On direct comparison of **6** with $[Zr\{Me_2Si(\eta^5\text{-}C_5Me_4)(\eta^5\text{-}C_5H_4)\}Cl_2]$ (Cent–Zr–Cent 128.10° [7a]) one can envisage a slight closing of the Cent–Zr–Cent angle on changing the substituent from methyl to phenyl. However, comparing **7** with $[Zr\{Me_2Si(\eta^5\text{-}C_5Me_4)(\eta^5\text{-}C_5H_3Pr^i)\}Cl_2]$ (Cent–Zr–Cent 126.9° [7b]) one can equally propose that the substituent has little effect on this angle. The Cl(1)–Zr(1)–Cl(2) angle (95.40(4)° and 93.65(4)° for **6** and **7**, respectively) is somewhat smaller than those recorded for the tetramethyl-substituted *ansa*-zirconocene complexes (Table 2).

As expected, the proximity of the phenyl groups in this system causes them to bend out of the C_5 plane away from the zirconium centre. The complete list of angles between the mean planes of the C_5 and C_6 units is given in Table 3.

Table 3
Angles between the phenyl and cyclopentadienyl planes and selected torsion angles in **6** and **7**

	6	**7**
Ph(1)	79.69	57.60
Ph(2)	41.24	64.83
Ph(3)	44.67	48.22
Ph(4)	59.40	65.76
C(1)–C(2)–C(21)–C(22)	70.0(3)	52.0(4)
C(1)–C(2)–C(21)–C(26)	−108.2(3)	−130.8(4)
C(2)–C(3)–C(31)–C(32)	132.6(3)	56.2(4)
C(2)–C(3)–C(31)–C(36)	−42.2(4)	−122.3(4)
C(3)–C(4)–C(41)–C(42)	128.6(3)	−50.2(4)
C(3)–C(4)–C(41)–C(46)	−45.3(4)	125.5(3)
C(4)–C(5)–C(51)–C(52)	−65.9(3)	−71.5(4)
C(4)–C(5)–C(51)–C(56)	116.1(3)	109.6(4)

Ph(1) refers to phenyl group formed by C(11)–C(16), Ph(2) to C(21)–C(26), Ph(3) to C(31)–C(36) and Ph(4) to C(41)–C(46).

2.1. Polymerization studies

Compounds **6** and **7** have been tested as catalysts in the polymerization of ethylene and compared with their tetramethyl-substituted analogues $[Zr\{Me_2Si(\eta^5\text{-}C_5Me_4)(\eta^5\text{-}C_5H_3R)\}Cl_2]$ (R = H (**8**); Bu^t (**9**)) and the reference catalyst $[Zr(\eta^5\text{-}C_5H_5)_2Cl_2]$. The polymerization experiments were carried out during 15 min with a MAO cocatalyst–metal catalyst ratio of 1000:1 at 20 °C and at olefin pressure of 2 bar. Under these conditions **6** and **7** were catalytically inactive, whilst the tetramethyl-substituted complexes **8** and **9** showed moderate activities compared with the reference catalyst (Table 4). The polymerization experiments were repeated varying the MAO cocatalyst–metal catalyst ratio (3000:1) and temperature (0 and 60 °C) and again **6** and **7** proved to be inactive.

Variable temperature NMR experiments, performed on **7**, have demonstrated that the phenyl substituents rotate

Table 4
Ethylene polymerization results for **6**–**9** and $[Zr(\eta^5\text{-}C_5H_5)_2Cl_2]$[a]

Catalyst	Activity[b]
$[Zr(\eta^5\text{-}C_5H_5)_2Cl_2]$	11 360
$[Zr\{Me_2Si(\eta^5\text{-}C_5Ph_4)(\eta^5\text{-}C_5H_4)\}Cl_2]$ (**6**)	0
$[Zr\{Me_2Si(\eta^5\text{-}C_5Ph_4)(\eta^5\text{-}C_5H_3Bu^t)\}Cl_2]$ (**7**)	0
$[Zr\{Me_2Si(\eta^5\text{-}C_5Me_4)(\eta^5\text{-}C_5H_4)\}Cl_2]$ (**8**)	2185
$[Zr\{Me_2Si(\eta^5\text{-}C_5Me_4)(\eta^5\text{-}C_5H_3Bu^t)\}Cl_2]$ (**9**)	1490

[a] At 20 °C, 2 bar ethylene pressure, 200 mL toluene, $[Al] = 3 \times 10^{-2}$ mol L^{-1}, $[Zr] = 3 \times 10^{-5}$ mol L^{-1}, $t_{Pol} = 15$ min.
[b] In kg Pol (mol Zr h bar)$^{-1}$.

almost unhindered above 0 °C, probably blocking the Cl–Zr–Cl plane, as has previously been proposed for the *ansa*-zirconocene complex $[Zr\{(CH_2CHPh)(\eta^5\text{-}C_5Ph_4)(\eta^5\text{-}C_5H_4)\}Cl_2]$ [5c]. Nevertheless, this complex showed a slight activity at 80 °C. Thus, a final polymerization experiment was performed at this temperature with **6** or **7** and yet again the complexes were not active.

Polymerization of ethylene was not observed when using the co-catalyst $B(C_6F_5)_3$ with the dimethyl derivatives of **6** and **7**.

2.2. Computational analysis of the catalytic behaviour of tetraphenyl-substituted ansa-zirconocene complexes

In order to explain the inactivity of the catalysts **6** and **7** in the polymerization of ethylene, a density functional theory (DFT) study has been carried out (see Section 4 for calculation details). Throughout this analysis, it is assumed that the active species for olefin polymerization are "naked" cationic or ionic-pair catalyst/co-catalyst species in which both chloride atoms have been substituted by methyl groups, one of which is subsequently extracted by a co-catalyst reagent creating a vacant site where monomer coordination takes place [10]. We have explored two different mechanisms which may explain the lack of activity of the catalysts **6** and **7**. Firstly, an interaction between phenyl ligands linked to the cyclopentadienyl moiety and the metal centre in the polymerization active species. Some similar interactions calculated by DFT methods between ancillary ligands and metal site have been previously shown to influence polymerization mechanisms [11]. Secondly, the influence of the bulky ancillary ligands on the formation of ion-pair active species by two different co-catalyst models; a six-member cage of MAO and $B(C_5F_6)_3$.

Two distinct structures were found by DFT geometrical optimization for the "naked" cationic active species of catalyst **7** (Fig. 3). Distances and angles for both geometries are given in the Supporting Information. Root mean square deviations (rmsd) of selected distances and angles between the experimental (**7**) and the optimized structures (**7a**) show a very good agreement (rmsd of 4 pm for distances and 1.6° for angles). A structure in which a η^2 interaction between a phenyl group and the zirconium atom of the active catalytic species has been found (**7b**, Fig. 3). One of the phenyl substituents is close to the metal atom (distances Zr(1)–C(51) = 288.4 pm and Zr(1)–C(52) = 287.6 pm) hindering the coordination of the monomer to the vacant site. Further evidence for the existence of an η^2 interaction is a slight stretching of the C(51)–C(52) bond distance (141.9 pm) with respect to the other C–C bonds in the same ring (139.5–140.5 pm) and equivalent bonds in the other phenyl ligands (140.9–140.5 pm) (for further distances see Supporting Information). However, this conformation is only 0.4 kcal/mol more stable than the structure found with no η^2 interaction between phenyl and metal centre (**7a**, Fig. 3). Thus, we can assume that both conformers are likely to be present during the polymerization reaction. In light of these results, it seems that further studies of monomer complexation and subsequent insertion in **7a** and **7b** are probably not relevant. It

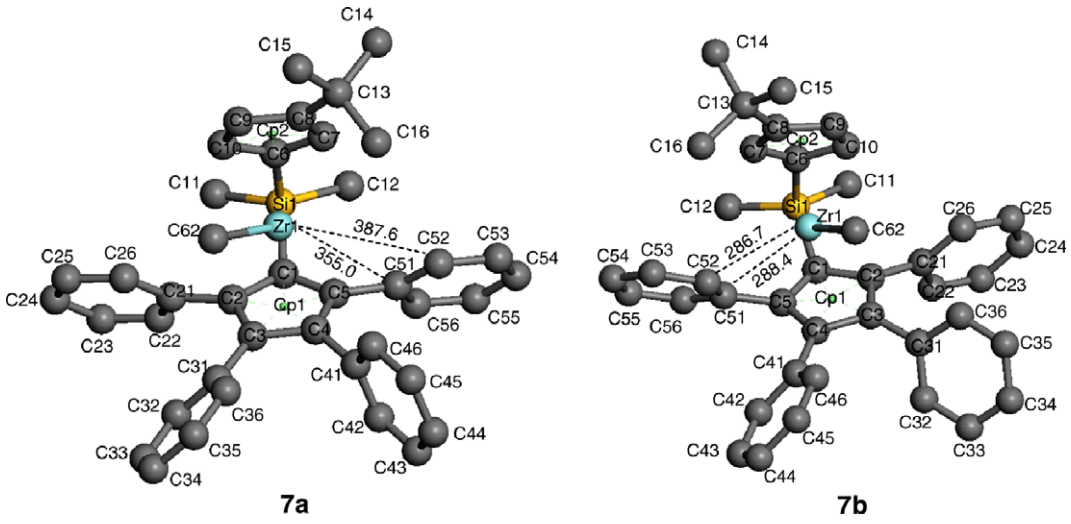

Fig. 3. Conformations for the cationic species of catalyst **7**. Structure **7b** shows an η^2 interaction. For clarity, hydrogen atoms are not shown. Distances are given in picometres. Numbering of atoms is the same as in Fig. 2.

is therefore apparent that this argument is not able to give an adequate reason for the lack of catalytic activity of the tetraphenyl-substituted complexes.

We have explored another possible mechanism which could explain the experimental results, namely the influence of the ancillary phenyl groups in the methyl extraction process from the dimethyl catalyst precursor by action of the co-catalyst. This step corresponds to formation of ion-pair active species on which would take place the chain growth. We have adopted two distinct models, a six-membered AlMeO cage activated by the presence of $AlMe_3$ and $B(C_6F_5)_3$ as cocatalysts [10]. In the same way, two catalysts were chosen, one substituted and inactive ([Zr{$Me_2Si(\eta^5$-$C_5Ph_4)(\eta^5$-$C_5H_3Bu^t)$}Me_2] (**7**)) and the other unsubstituted and catalytically active in ethylene polymerization ([Zr{$Me_2Si(\eta^5$-$C_5H_4)_2$}Me_2] (**10**) [12]). The optimized structures of the substituted (**7**) and the unsubstituted catalysts (**10**) involved in the formation of the ion-pair active

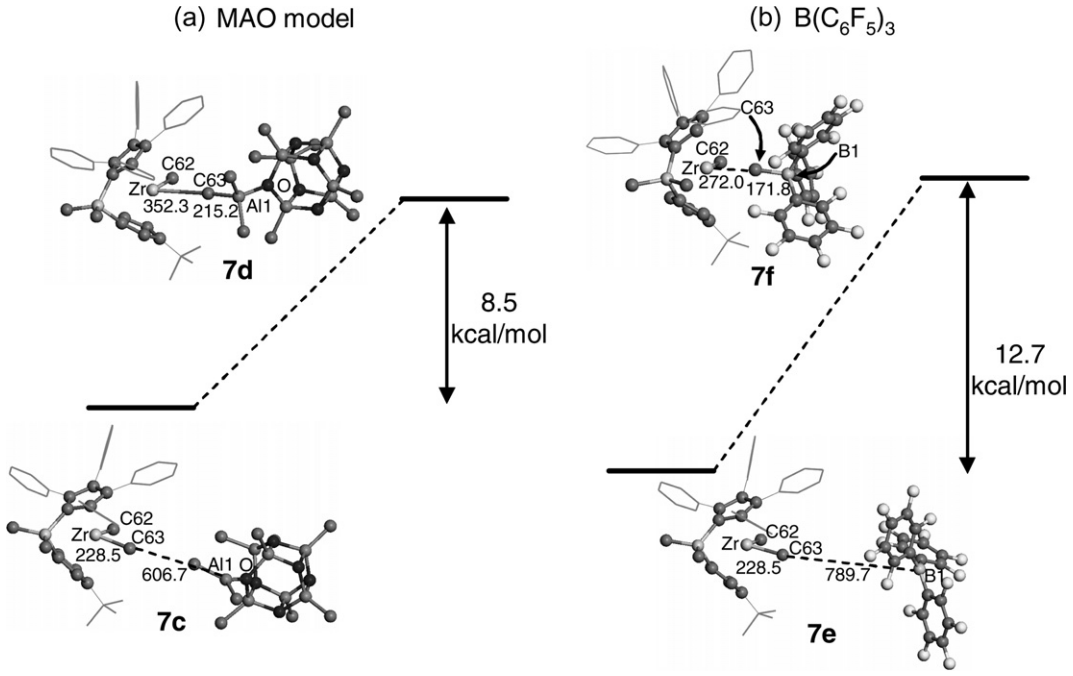

Fig. 4. Relative stability of reaction intermediates corresponding to methyl extraction by six-cage MAO model and $B(C_6F_5)_3$ cocatalysts from precatalyst [Zr{$Me_2Si(\eta^5$-$C_5Ph_4)(\eta^5$-$C_5H_3Bu^t)$}Me_2] (**7**). Phenyl and *tert*-butyl groups are displayed as lines and hydrogen atoms are not shown for the sake of clarity.

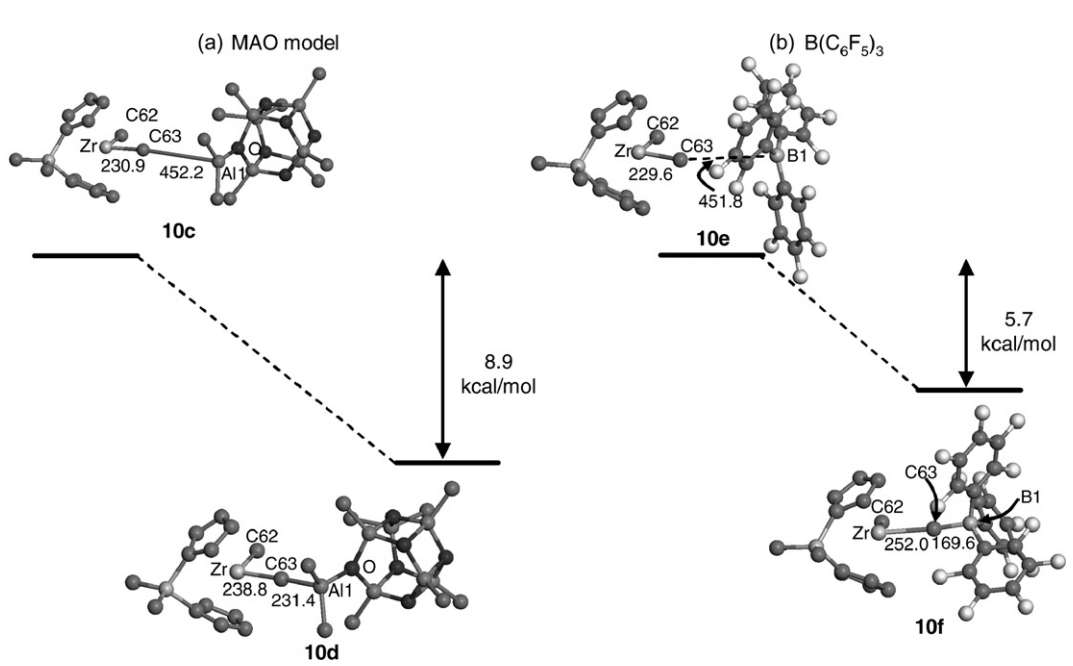

Fig. 5. Relative stability of reaction intermediates corresponding to methyl extraction by six-cage MAO model and $B(C_6F_5)_3$ cocatalysts from precatalyst [Zr{$Me_2Si(\eta^5$-$C_5H_4)_2$}Me_2] (**10**). Hydrogen atoms are not shown for the sake of clarity.

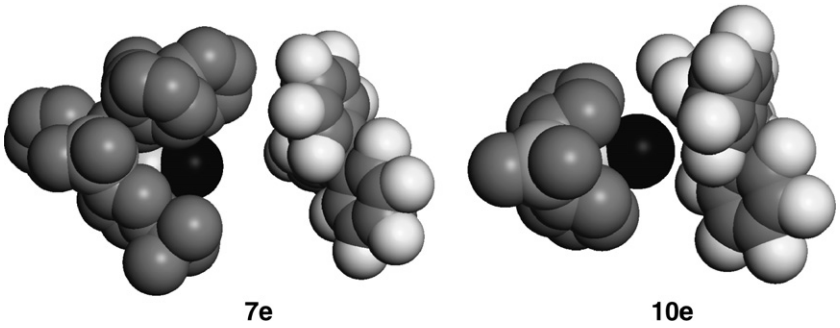

Fig. 6. Van der Waals molecular model for ion-pair **7e** and **10e** precursors (defined in Figs. 4 and 5). The black ball represents the methyl group to be extracted by the co-catalyst. Hydrogen atoms are not shown for the sake of clarity.

species for both co-catalysts are shown in Figs. 4 and 5, respectively. It was observed that the extraction of a methyl group to form the cationic active species are endothermic for both **7/MAO** and **7/B(C_6F_5)$_3$** systems (8.5 and 12.7 kcal/mol, respectively, see Fig. 4), whilst for the unsubstituted analogue systems the formation of the cation are exothermic (8.9 and 5.7 kcal/mol, see Fig. 5). Thus, formation of the ionic-pair active species is not favourable in the case of the bulky catalyst **7**. Endothermic process for the ion-pair formation of these catalysts may be explained using steric arguments. The steric effect can be visualized using Van der Waals radii for the ion-pair **7e** and **10e** precursors as shown in Fig. 6. As can be seen, the methyl groups in catalyst **7** are sterically hindered by the phenyl and *tert*-butyl groups linked to the cyclopentadienyl moieties, therefore the approach of an incoming co-catalyst molecule to extract a methyl group and to create a vacant site is restricted. Thus, the formation of the catalytically active species is unlikely. However, the steric pressure is alleviated in the unsubstituted catalyst **10** and consequently the formation of the required ion-pair for the polymerization reaction is favourable.

3. Conclusions

We have synthesized and structurally characterized the *ansa*-zirconocene complexes [Zr{$Me_2Si(\eta^5$-$C_5Ph_4)(\eta^5$-$C_5H_3R)$}Cl_2] (R = H, Bu^t). We have demonstrated that these complexes are inactive as catalysts in ethylene polymerization. DFT calculations showed that the interaction of the ancillary ligands with the metal centre cannot explain the lack of activity of the phenyl-substituted catalysts. We have found that steric hindrance, caused by the tetraphenyl moiety, in the co-catalyst induced methyl extraction step is responsible for the unfavourable formation of the suitable ion-pair active species.

4. Experimental

4.1. Materials and procedures

All reactions were performed using standard Schlenk tube techniques in an atmosphere of dry nitrogen. Solvents were distilled from the appropriate drying agents and degassed before use. $SiMe_2Cl_2$, $C_5H_2Ph_4$, Li($C_5H_4Bu^t$), MAO (10% wt in toluene), $ZrCl_4$ and [Zr(η^5-$C_5H_5)_2Cl_2$] were purchased from Aldrich and used without further purification. Na(C_5H_5) [13], Li(C_5HPh_4) [14] and [Zr{Me_2-Si(η^5-C_5Me_4)(η^5-C_5H_3R)}Cl_2] (R = H [7a], Bu^t [7b]) were prepared as previously reported. ^{1}H and ^{13}C{^{1}H} spectra were recorded on a Varian Mercury FT-400 spectrometer or on a Bruker AVANCE-400 and referenced to the residual deuterated solvent. Microanalyses were carried out with a Perkin–Elmer 2400 microanalyzer. Mass spectroscopic analyses were preformed on a Hewlett–Packard 5988A (*m*/*z* 50–1000) instrument.

Table 5
Crystal data and structure refinement for **6** and **7**

	6	**7**
Formula	$C_{36}H_{30}Cl_2SiZr$	$C_{40}H_{38}Cl_2SiZr$
F_w	652.81	708.91
T (K)	130(2)	130(2)
Crystal system	Triclinic	Monoclinic
Space group	$P\bar{1}$	$P2(1)/n$
a (pm)	975.3(5)	990.89(2)
b (pm)	1018.9(5)	2645.98(4)
c (pm)	1736.6(5)	1303.95(2)
α (°)	96.364(5)	90
β (°)	100.519(5)	105.337(2)
γ (°)	117.718(5)	90
V (nm^3)	1.4635(11)	3.29704(10)
Z	2	4
D_c (Mg m^{-3})	1.481	1.428
μ (mm^{-1})	0.624	0.560
F(000)	668	1464
Crystal dimensions (mm)	0.3 × 0.1 × 0.05	0.5 × 0.2 × 0.2
θ Range (°)	2.63–26.02	2.63–28.28
hkl ranges	$-11 \geqslant h \geqslant 12$, $-12 \leqslant k \leqslant 12$, $-21 \leqslant l \leqslant 21$	$-13 \leqslant h \leqslant 13$, $-35 \leqslant k \leqslant 35$, $-17 \leqslant l \leqslant 17$
Data/parameters	5734/363	8188/402
Goodness-of-fit on F^2	0.853	1.034
Final R indices [$I > 2\sigma(I)$]	0.0304	0.0579
R indices (all data)	0.0578	0.0687
Largest difference in peak and hole (e Å^{-3})	0.528 and −0.309	4.872 and −1.973

$R_1 = \sum||F_o| - |F_c||/\sum|F_o|$; $wR_2 = [\sum[w(F_o^2 - F_c^2)^2]/\sum[w(F_o^2)^2]]^{0.5}$.

4.2. Data collection and structural refinement of 6 and 7

The data of **6** and **7** were collected with a CCD Oxford Xcalibur S (λ(Mo Kα) = 0.71073 Å) using ω and φ scans mode. Semi-empirical from equivalents absorption corrections were carried out with SCALE3 ABSPACK [15]. All the structures were solved by direct methods [16]. Structure refinement was carried out with SHELXL-97 [17]. All non-hydrogen atoms were refined anisotropically, and hydrogen atoms were located by difference maps and refined isotropically. Table 5 lists crystallographic details.

4.3. Synthesis of $C_5HPh_4(SiMe_2Cl)$ (1)

$SiMe_2Cl_2$ (1.44 g, 11.16 mmol) in THF (50 mL) was added to a solution of $Li(C_5HPh_4)$ (1.40 g, 3.72 mmol) in THF (50 mL) at −78 °C. The reaction mixture was allowed to warm to room temperature and stirred for 15 h. Solvent was removed under vacuum and toluene (100 mL) was added to the resulting dark yellow oil. The mixture was filtered and solvent removed, from the filtrate, under reduced pressure to yield the title compound as a dark yellow solid. Yield 1.58 g, 92%. ^{1}H NMR (400 MHz, $CDCl_3$; for the predominant isomer): δ −0.15 (s, 6H, Si*Me*$_2$), 4.16 (br, 1H, C_5H), 6.88–7.21 (m, 20H, *Ph*). MS electron impact (*m*/*e* (% relative intensity)): 463 (14) [M^+], 427 (40) [M^+−Cl], 369 (98) [M^+−ClSiMe$_2$]. Anal. Calc. for $C_{31}H_{27}ClSi$: C, 80.40; H, 5.88. Found: C, 80.59; H, 5.84%.

4.4. Synthesis of $Me_2Si(C_5HPh_4)(C_5H_5)$ (2)

$C_5HPh_4(SiMe_2Cl)$ (**1**) (1.50 g, 3.24 mmol) in THF (50 mL) was added to a solution of $Na(C_5H_5)$ (0.28 g, 3.24 mmol) in THF (50 mL) at −78 °C. The reaction mixture was allowed to warm to room temperature and stirred for 15 h. Solvent was removed in vacuo and toluene (120 mL) was added to the resulting dark orange oil. The mixture was filtered and solvent removed, from the filtrate, under reduced pressure to yield the title compound as an orange oil (1.38 g, 86%). ^{1}H NMR (400 MHz, $CDCl_3$; for the predominant isomer): δ −0.10 (s, 6H, Si*Me*$_2$), 3.20 (1H), 4.12 (1H) (m, *H*C$_5$), 5.02 (2H), 5.35 (2H) (m, C_5H_4), 6.91–7.17 (m, 20H, *Ph*). MS electron impact (*m*/*e* (relative intensity)): 492 (21) [M^+], 427 (23) [M^+−C_5H_4], 370 (72) [M^+−$C_5H_5SiMe_2$], 123 (100) [M^+−C_5HPh_4]. Anal. Calc. for $C_{36}H_{32}Si$: C, 87.75; H, 6.55. Found: C, 87.51; H, 6.48%.

4.5. Synthesis of $Me_2Si(C_5HPh_4)(C_5H_4Bu^t)$ (3)

The synthesis of **3** was carried out in an identical manner to **2**. $C_5HPh_4(SiMe_2Cl)$ (**1**) (1.50 g, 3.24 mmol) in THF (50 mL) and $Li(C_5H_4Bu^t)$ (0.40 g, 3.24 mmol). Yield: 0.75 g, 84%. ^{1}H NMR (400 MHz, $CDCl_3$; for the predominant isomer): δ 0.28 (s, 6H, Si*Me*$_2$), 0.99 (s, 9H, Bu^t), 3.12 (1H), 3.62 (1H) (m, *H*C$_5$), 6.01 (1H), 6.18 (1H), 6.38 (1H) (m, C_5H_3), 6.95–7.14 (m, 20H, *Ph*). MS electron impact (*m*/*e* (relative intensity)): 548 (29) [M^+], 462 (71) [M^+−Bu^t−2×Me], 399 (51) [M^+−Bu^t−Me−Ph], 179 (33) [M^+−C_5Ph_4]. Anal. Calc. for $C_{40}H_{40}Si$: C, 87.54; H, 7.35. Found: C, 87.21; H, 7.23%.

4.6. Synthesis of $Li\{Me_2Si(C_5Ph_4)(C_5H_4)\}$ (4)

LiBu^n (1.6 M in hexane) (1.65 mL, 2.64 mmol) was added dropwise to a solution of $Me_2Si(C_5Ph_4)(C_5H_5)$ (**2**) (0.65 g, 1.32 mmol) in Et_2O (100 mL) at −78 °C. The mixture was allowed to warm to room temperature and stirred for 15 h. Solvent was removed in vacuo to give a white solid which was washed with hexane (2 × 50 mL) and dried under vacuum. Yield: 0.61 g, 91%. Anal. Calc. for $C_{36}H_{30}Li_2Si$: C, 86.59; H, 5.99. Found: C, 86.25; H, 5.78%.

4.7. Synthesis of $Li\{Me_2Si(C_5Ph_4)(C_5H_3Bu^t)\}$ (5)

The synthesis of **5** was carried out in an identical manner to **4**. LiBu^n (1.6 M in hexane) (1.60 mL, 2.56 mmol) and $Me_2Si(C_5HPh_4)(C_5H_4Bu^t)$ (**3**) (0.70 g, 1.28 mmol). Yield: 0.65 g, 91%. Anal. Calc. for $C_{40}H_{38}Li_2Si$: C, 85.68; H, 6.83. Found: C, 85.31; H, 6.72%.

4.8. Synthesis of $[Zr\{Me_2Si(\eta^5\text{-}C_5Ph_4)(\eta^5\text{-}C_5H_4)\}Cl_2]$ (6)

$Li_2\{Me_2Si(C_5Ph_4)(C_5H_4)\}$ (**4**) (0.55 g, 1.10 mmol) in THF (50 mL) was added dropwise during 15 min to a solution of $ZrCl_4$ (0.13 g, 0.55 mmol) in THF (50 mL) at 0 °C. The reaction mixture was allowed to warm to room temperature and stirred under reflux for 18 h. Solvent was removed in vacuo and toluene (120 mL) added to the resulting solid. The mixture was filtered and the filtrate concentrated (20 mL) and cooled to −30 °C to give crystals of the title complex. Yield: 0.26 g, 44%. ^{1}H NMR (400 MHz, $CDCl_3$): δ 0.16 (s, 6H, Si*Me*$_2$), 5.02 (2H), 5.48 (2H) (m, C_5H_4), 6.90–7.19 (m, 20H, *Ph*). ^{13}C{^{1}H} NMR (100 MHz, $CDCl_3$): δ 2.8 (Si*Me*$_2$), 100.3, 101.2 (C^1-Cp), 109.2, 114.3 (C_5H_4), 123.1, 125.7 (C_5Ph_4), 127.3, 128.4, 129.7, 130.5, 131.2, 133.9, 141.1, 143.2 (*Ph*). MS electron impact (*m*/*e* (relative intensity)): 652 (90) [M^+], 617 (33) [M^+−Cl], 582 (100) [M^+−2×Cl]. Anal. Calc. for $C_{36}H_{30}Cl_2SiZr$: C, 66.23; H, 4.63. Found: C, 66.08; H, 4.54%.

4.9. Synthesis of $[Zr\{Me_2Si(\eta^5\text{-}C_5Ph_4)(\eta^5\text{-}C_5H_3Bu^t)\}Cl_2]$ (7)

The synthesis of **7** was carried out in an identical manner to **6**. $Li_2\{Me_2Si(C_5Ph_4)(C_5H_3Bu^t)\}$ (**5**) (0.60 g, 1.07 mmol) and $ZrCl_4$ (0.25 g, 1.07 mmol). Yield: 0.36 g, 48%. ^{1}H NMR (400 MHz, $CDCl_3$): δ 0.14 (3H), 0.62 (3H) (s, Si*Me*$_2$), 1.01 (s, 9H, *Bu*^{t}), 5.80 (1H), 5.93 (1H), 6.96 (1H) (m, C_5H_3), 6.98–7.19 (m, 20H, *Ph*). ^{13}C{^{1}H} NMR (100 MHz, $CDCl_3$): δ 3.7, 4.6 (Si*Me*$_2$), 27.2, 38.4 (*Bu*^{t}), 92.8, 100.1 (C^1-Cp), 109.1, 111.4, 116.3, 120.6 (C_5H_3),

123.2, 131.0, 133.1, 136.7 (C_5Ph_4), 126.5, 127.4, 128.6, 130.8, 133.5, 143.0, 145.2, 145.5 (*Ph*). MS electron impact (*m*/*e* (relative intensity)): 709 (67) [M^+], 673 (8) [M^+-Cl], 617 (49) [$M^+-Cl-Bu^t$], 587 (55) [$M^+-Cl-Bu^t-2\times Me$]. Anal. Calc. for $C_{40}H_{38}Cl_2SiZr$: C, 67.77; H, 5.40. Found: C, 67.30; H, 5.31%.

4.10. Polymerization of ethylene

The zirconocene catalyst (6 μmol), MAO (10% in toluene) (6000 μmol) and toluene (200 mL) were mixed together for 15 min in a 1 l glass autoclave. The N_2 pressure inside the autoclave was reduced by applying vacuum. Ethylene pressure of 2 bar was then applied and maintained to the autoclave and stirring of the mixture commenced (1000 rpm). After exactly 15 min, stirring was halted and the ethylene pressure released. Excess MAO was then destroyed by adding cautiously a mixture of methanol/HCl (90:10). The polymer was isolated by filtration and washed with ethanol and dried under vacuum at 90 °C for 16 h.

4.11. Theoretical calculations

The Becke 1988 [18] for exchange and Perdew 1986 [19] for correlation gradient corrected functional were used for all the geometry optimization calculations. We selected a double zeta quality numerical basis set which included polarization (DZP) for all atoms including hydrogen atoms [20]. For the Zr metal atom a pseudopotential [21] was used. All the calculations were carried out with the DMOL [20,22] package included in the MATERIALSSTUDIO [23] software.

Acknowledgements

We gratefully acknowledge financial support from the Ministerio de Educación y Ciencia, Spain (Grants numbers CTQ2005-07918-C02-02/BQU and MAT2006-400), the Comunidad de Madrid (S-0505/PPQ-0328), the Universidad Rey Juan Carlos (graduate fellowship for D. Polo-Cerón) and the Alexander von Humboldt-Stiftung (Humboldt-Fellowship for S. Gómez-Ruiz). J. Ramos thanks CSIC for financial support through an I3P tenure track.

Appendix A. Supplementary material

CCDC 658048 and 658049 contain the supplementary crystallographic data for this paper. These data can be obtained free of charge from The Cambridge Crystallographic Data Centre via www.ccdc.cam.ac.uk/data_request/cif. PDB files of the calculated structures are provided as supplementary material. Supplementary data associated with this article can be found, in the online version, at doi:10.1016/j.jorganchem.2007.11.054.

References

[1] (a) N.J. Long, Metallocenes. An Introduction to Sandwich Complexes, Blackwell Science Ltd., Oxford, 1998;
(b) A. Togni, Metallocenes, Wiley–VCH, Weinheim, 1998.
[2] (a) M.P. Castellani, J.M. Wright, S.J. Geib, A.L. Rheingold, W.C. Trogler, Organometallics 5 (1986) 1116;
(b) F.O. Arp, G.C. Fu, J. Am. Chem. Soc. 128 (2006) 14264;
(c) R. Peters, Z.-Q. Xin, D.F. Fischer, W.B. Schweizer, Organometallics 25 (2006) 2917;
(d) H. Schumann, K. Suehring, Z. Naturforsch B 60 (2005) 383;
(e) I.D. Hills, G.C. Fu, Angew. Chem., Int. Ed. 42 (2003) 3921;
(f) A.H. Mermerian, G.C. Fu, J. Am. Chem. Soc. 125 (2003) 4050;
(g) J. Norinder, H.K. Cotton, J.-E. Baeckvall, J. Org. Chem. 67 (2002) 9096.
[3] M.P. Castellani, S.J. Geib, A.L. Rheingold, W.C. Trogler, Organometallics 6 (1987) 1703.
[4] M.P. Castellani, S.J. Geib, A.L. Rheingold, W.C. Trogler, Organometallics 6 (1987) 2524.
[5] (a) U. Thewaldt, G. Schmidt, J. Organomet. Chem. 412 (1991) 343;
(b) B. Rieger, T. Repo, G. Jany, Polymer Bull. 35 (1995) 87;
(c) B. Rieger, M. Steinmann, R. Fawzi, Chem. Ber. 125 (1992) 2373;
(d) D.L. Greene, A. Chau, M. Monreal, C. Mendez, I. Cruz, T. Wenj, W. Tikkanen, B. Schick, K. Kantardjieff, J. Organomet. Chem. 682 (2003) 8;
(e) J. An, L. Urrieta, R. Williams, W. Tikkanen, R. Bau, M. Yousufuddin, J. Organomet. Chem. 690 (2005) 4376;
(f) D.L. Green, O.A. Villalta, D.M. Macias, A. Gonzalez, W. Tikkanen, B. Schick, K. Kantardjieff, Inorg. Chem. Commun. 2 (1999) 311;
(g) S.-S. Xu, F. Yuan, S.-S. He, B.-Q. Wang, X.-Z. Zhou, F.-L. Zou, Y. Li, Youji Huaxue 23 (2003) 187;
(h) A. Altomare, F. Ciardelli, N. Tirelli, R. Solaro, Macromolecules 30 (1997) 1298;
(i) F. Ciardelli, A. Altomare, G. Arribas, G. Conti, F. Masi, F. Menconi, Stud. Surf. Sci. Catal. 89 (1994) 257;
(j) G. Conti, G. Arribas, A. Altomare, B. Mendez, F. Ciardelli, Z. Naturforsch., B: Chem. Sci. 50 (1995) 411;
(k) D.W. Stephan, J.C. Stewart, F. Guerin, S. Courtenay, J. Kickham, E. Hollink, C. Beddie, A. Hoskin, T. Graham, P. Wei, R.E. Spence, W. Xu, L. Koch, X. Gao, D.G. Harrison, Organometallics 22 (2003) 1937;
(l) S. Barry, A. Kucht, H. Kucht, M.D. Rausch, J. Organomet. Chem. 489 (1995) 195;
(m) A. Kucht, H. Kucht, S. Barry, J.C.W. Chien, M.D. Rausch, Organometallics 12 (1993) 3075;
(n) K.H. Thiele, F. Rehbaum, H. Baumann, H. Schumann, F.H. Goerlitz, R. Weimann, Z. Anorg. Allgem. Chem. 613 (1992) 76.
[6] See for example: (a) L. Resconi, L. Cavallo, A. Fait, F. Piemontesi, Chem. Rev. 100 (2000) 1253;
(b) H.H. Brintzinger, D. Fischer, R. Mülhaupt, B. Rieger, R.M. Waymouth, Angew. Chem., Int. Ed. Engl. 36 (1995) 1143;
(c) J. Zhang, X. Wang, G.-X. Jin, Coord. Chem. Rev. 250 (2006) 95;
(d) S. Prashar, A. Antiñolo, A. Otero, Coord. Chem. Rev. 250 (2006) 133;
(e) B. Wang, Coord. Chem. Rev. 250 (2006) 242;
(f) P.C. Möhring, N.J. Coville, Coord. Chem. Rev. 250 (2006) 18.
[7] (a) A. Antiñolo, I. López-Solera, I. Orive, A. Otero, S. Prashar, A.M. Rodríguez, E. Villaseñor, Organometallics 20 (2001) 71;
(b) A. Antiñolo, I. López-Solera, A. Otero, S. Prashar, A.M. Rodríguez, E. Villaseñor, Organometallics 21 (2002) 2460;
(c) A. Antiñolo, M. Fajardo, S. Gómez-Ruiz, I. López-Solera, A. Otero, S. Prashar, A.M. Rodríguez, J. Organomet. Chem. 683 (2003) 11;
(d) A. Antiñolo, M. Fajardo, S. Gómez-Ruiz, I. López-Solera, A. Otero, S. Prashar, Organometallics 23 (2004) 4062;
(e) S. Gómez-Ruiz, S. Prashar, M. Fajardo, A. Antiñolo, A. Otero, M.A. Maestro, V. Volkis, M.S. Eisen, C.J. Pastor, Polyhedron 24 (2005) 1298;

(f) S. Gómez-Ruiz, S. Prashar, L.F. Sánchez-Barba, D. Polo-Cerón, M. Fajardo, A. Antiñolo, A. Otero, M.A. Maestro, C.J. Pastor, J. Mol. Catal. A: Chem. 264 (2007) 260;
(g) D. Polo-Cerón, S. Gómez-Ruiz, S. Prashar, M. Fajardo, A. Antiñolo, A. Otero, I. López-Solera, M.L. Reyes, J. Mol. Catal. A: Chem. 268 (2007) 264;
(h) D. Polo-Cerón, S. Gómez-Ruiz, S. Prashar, M. Fajardo, A. Antiñolo, A. Otero, Collect. Czech. Chem. Commun. 72 (2007) 747;
(i) V.L. Cruz, S. Martinez, J. Martinez-Salazar, D. Polo-Cerón, S. Gómez-Ruiz, M. Fajardo, S. Prashar, Polymer 48 (2007) 4663;
(j) S. Gómez-Ruiz, D. Polo-Cerón, S. Prashar, M. Fajardo, A. Antiñolo, A. Otero, Eur. J. Inorg. Chem. 2007 (2007) 4445.

[8] (a) M.A. Giardello, M.S. Eisen, C.L. Stern, T.J. Marks, J. Am. Chem. Soc. 115 (1993) 3326;
(b) M.A. Giardello, M.S. Eisen, C.L. Stern, T.J. Marks, J. Am. Chem. Soc. 117 (1995) 12114.

[9] T. Koch, S. Blaurock, F.B. Somoza, A. Voigt, R. Kirmse, E. Hey-Hawkins, Organometallics 19 (2000) 2556.

[10] (a) E. Zurek, T. Ziegler, Prog. Polym. Sci. 29 (2004) 101;
(b) E. Zurek, T. Ziegler, Organometallics 21 (2002) 83;
(c) S. Martinez, J. Ramos, V.L. Cruz, J. Martinez-Salazar, Polymer 47 (2006) 883.

[11] V.L. Cruz, S. Martinez, J. Martinez-Salazar, J. Sancho, Macromolecules 40 (2007) 7413.

[12] V. Cruz, J. Ramos, A. Muñoz-Escalona, P. Lafuente, B. Peña, J. Martinez-Salazar, Polymer 45 (2004) 2061.

[13] T.K. Panda, M.T. Gamer, P.W. Roesky, Organometallics 22 (2003) 877.

[14] R. Zhang, M. Tsutsui, D.E. Bergbreiter, J. Organomet. Chem. 229 (1982) 109.

[15] SCALE3 ABSPACK: Empirical Absorption Correction, CrysAlis – Software package, Oxford Diffraction Ltd., 2006.

[16] G.M. Sheldrick, SHELXS-97, Program for Crystal Structure Solution, Göttingen, 1997.

[17] G.M. Sheldrick, SHELXL-97, Program for the Refinement of Crystal Structures, Göttingen, 1997.

[18] A.D. Becke, Phys. Rev. A 38 (1988) 3098.

[19] J.P. Perdew, Phys. Rev. B 33 (1986) 8822.

[20] B. Delley, J. Chem. Phys. 92 (1990) 508.

[21] (a) M. Dolg, U. Wedig, H. Stoll, H. Preuss, J. Chem. Phys. 86 (1987) 866;
(b) A. Bergner, M. Dolg, W. Kuechle, H. Stoll, H. Preuss, Mol. Phys. 80 (1993) 1431.

[22] B. Delley, J. Chem. Phys. 113 (2000) 7756.

[23] MATERIALSTUDIO version 4.1. Accelrys Inc., 2006.